

Article

The Influence of Base Metal (M) Oxidation State in Au-M-O/TiO₂ Systems on Their Catalytic Activity in Carbon Monoxide Oxidation

Jan Mizera, Nika Spiridis, Robert P. Socha, Małgorzata Zimowska, Ryszard Grabowski *, Katarzyna Samson and Józef Korecki

Jerzy Haber Institute of Catalysis and Surface Chemistry, Polish Academy of Sciences, Niezapominajek 8, Cracow 30-239, Poland; E-Mails: ncmizera@cyf-kr.edu.pl (J.M.); ncspirid@cyf-kr.edu.pl (N.S.); ncsocha@cyf-kr.edu.pl (R.P.S.); nczimows@cyf-kr.edu.pl (M.Z.); ncsamson@cyf-kr.edu.pl (K.S.); korecki@uci.agh.edu.pl (J.K.)

* Author to whom correspondence should be addressed; E-Mail: ncgrabow@cyf-kr.edu.pl; Tel.: +48-12-6395-161.

Received: 6 October 2011; in revised form: 5 November 2011 / Accepted: 7 December 2011 /

Published: 22 December 2011

Abstract: Base metal promoted gold/titania catalysts were synthesized, characterized and tested in CO oxidation reaction. Catalysts containing dopant metals in higher oxidation states exhibited higher activity than catalysts containing dopants in reduced states. The activity of fresh catalysts promoted by Cu, Fe and Ni was similar to the unpromoted one, but treatment in reducing and oxidizing atmospheres revealed the supremacy of the copper promoted catalyst. The sequential deposition method proved to be better than the co-deposition—precipitation method. An attempt to explain these differences using XPS, FTIR and H₂ TPR was performed.

Keywords: gold; CO oxidation; TiO₂; modifications

1. Introduction

It is hard to find a topic in the history of heterogeneous catalysis that has made such extreme progress over the last 20 years as is the case of gold catalysis. Regardless of the tiny harbingers published at the beginning of the 20th century [1,2] and the amazing discoveries presented in 1969 [3] and 1973 [4], until the mid of 1980s in the 20th century, scientists looked with disappointment at gold

as an element which was useful in catalysis only as a diluent for other noble metals [5]. However, since the revolutionary paper of Haruta [6] in 1987, only within a few years, fresh air could be enjoyed in Japanese hospitals and restrooms thanks to the applied catalytic converters, burning VOC's (Volatile Organic Compounds) on a Au/Fe₂O₃ catalyst bed [7,8] and some years later the first pilot plant for the gold catalyzed one-step direct production of methyl glycolate from ethylene glycol and methanol was started [9]. Until today the activity of gold nanoparticles in several dozens of reactions has been proven and the scientific world knows more and more about the laws of nature ruling the catalytic system. Nevertheless, the industry can hardly wait to see reliable research showing active and stable catalysts for CO oxidation.

The problem encumbering them is the relatively low time-on-stream stability caused by the reduction of the Au oxidation state and accumulation of carbonates and formates on the gold active sites [10]. The most common trend to solve these problems was changing the support materials from common ones (titania, iron oxides) into more expensive ones like zirconia and rare earth metal oxides [11]. Even if such an approach led to the discovery of general rules, describing the properties of a stable catalyst, these general rules would need to be further transferred into knowledge about tailoring stable catalysts with cheaper supports. Thus, it seems that tuning titania properties by doping it with other metal oxides appears to be a good shortcut on the way to discover an applicable gold catalyst. This approach seems to be reasonable not only because of the difference in prices of the mentioned supports, but also because of the possibility to use the ample knowledge that scientists already have about titania.

It was shown that the role of the support in gold catalysts is not limited to only being a material on which gold nanoparticles can be deposited. The intrinsic properties of the support, especially its reducibility, can influence the properties of gold nanoparticles such as the size and the electronic state [12,13]. Also these reducible supports generate more oxygen vacancies at the Au-support interface [14,15], which is believed to be the center activating oxygen molecules.

The idea of this research is to modify an active catalyst (Au/TiO₂) with metal oxides (Fe, Ni, Cu), having different reducibility and the ability to generate oxygen vacancies in TiO₂ to tune the interactions between gold nanoparticles and the support, leading to higher catalytic activity. The presented results approach some dependencies between the type of the applied doping metal, its oxidation state, and the changes in the catalytic performance of the promoted catalyst.

2. Results and Discussion

The synthesized catalysts and their basic properties are listed in Table 1. The nominal content of gold was 1 wt% in all cases and the content of base metals was always equimolar with respect to gold. In the case of Au₁/TiO₂ and its modifications the applied support—Titania—had a surface area of 22.4 m²g⁻¹ and BET measurements showed that the modifications have no influence on the specific surface area. In the case of the rest of the samples the BET surface area was 32 m²g⁻¹.

Table 1. Basic properties of the synthesized catalysts.

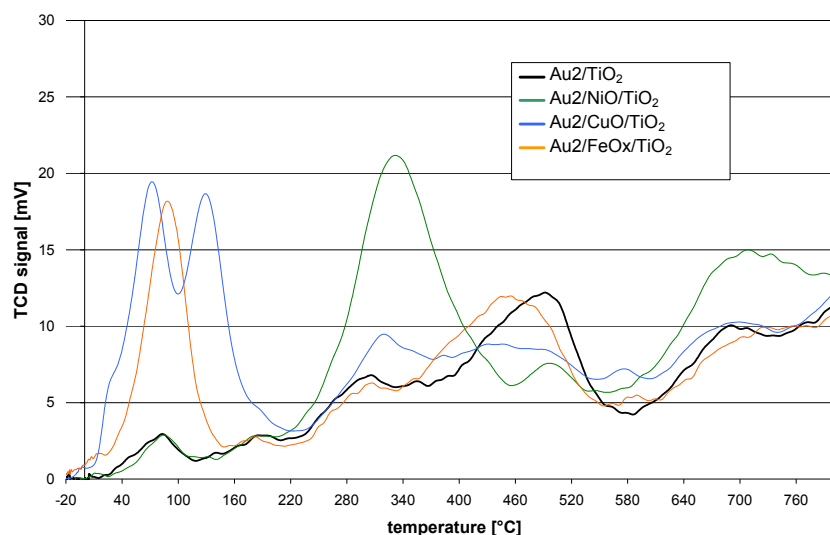
Catalyst	Preparation method		Nominal composition (wt%)		BET	TPR _{max}
	deposition	heating atmosphere (350 °C)	Au	M		
Au1/TiO ₂	DP *	air	1		22.4	–
NiO/Au1/TiO ₂	MaGSD *	air	1	0.3	22.4	–
Ni/Au1/TiO ₂	MaGSD *	5% H ₂ /Ar	1	0.3	22.4	–
Au1/NiO/TiO ₂	GaMSD *	air	1	0.3	22.4	–
Au1/Ni/TiO ₂	GaMSD *	5% H ₂ /Ar	1	0.3	22.4	–
Au2/TiO ₂	DP *	air	1		32	reference sample
Au2/NiO/TiO ₂	GaMSD *	air	1	0.3	32	340 °C
Au2/FeO _x /TiO ₂	GaMSD *	air	1	0.28	32	90 °C
Au2/CuO/TiO ₂	GaMSD *	air	1	0.32	32	70, 135 °C
Au3/TiO ₂	DP *	air	1		32	–
Au3 + NiO/TiO ₂	CoD *	air	1	0.3	32	–
Au3 + FeO _x /TiO ₂	CoD *	air	1	0.28	32	–
Au3 + CuO/TiO ₂	CoD *	air	1	0.32	32	–

* DP: Deposition Precipitation; MaGSD: Metal after Gold Sequential Deposition; GaMSD: Gold after Metal Sequential Deposition; CoD: Codeposition; Au1, Au2, Au3: Catalyst Series.

2.1. Catalyst Reducibility

The redox properties of the catalysts are shown in Figure 1. The course of the TPR curve of the reference catalyst (Au2/TiO₂) shows that the reduction starts just above room temperature. At further steps of the reduction process maxima can be observed at 90, 180, 300, 500 and 700 °C. The TPR curves of the promoted catalysts follow a similar course. However, they differ in the presence of additional reduction peaks, intensity or shift of the T_{max} with respect to the maxima observed for the reference catalyst.

Figure 1. TPR curves of catalysts obtained by sequential deposition of base metal oxides on TiO₂ followed by deposition of gold nanoparticles.



The Au₂/NiO/TiO₂ TPR curve is distinguished by the presence of a peak at 340 °C and also a lower intensity of that at 500 °C and higher intensity over 600 °C.

The Au₂/CuO/TiO₂ TPR profile revealed that the reduction process starts at −10 °C. Further temperature increase gives two low temperature peaks at 70 and 135 °C. Then at higher temperatures (300–400 °C) and also around 600 °C, the intensity of the peaks is higher while a lower intensity in the range 420–530 °C can be observed.

The TPR process of Au₂/FeO_x/TiO₂ starts at −15 °C. There is a well marked peak at 90 °C but none other at higher temperatures. Only the peak, observed for the reference catalyst at 500 °C, is slightly shifted by 40 °C towards lower temperatures in the case of the iron promoted catalyst.

The TPR curves presented in Figure 1 were integrated; the integral value of the reference catalyst (Au₂/TiO₂) was subtracted. On the basis of calibration data the amount of consumed hydrogen and the reduction degree was calculated. The values are shown in Table 2.

Table 2. Reduction degrees of promoted catalyst calculated from TPR curves.

Promoter	Ni			Fe	Cu
Presumed valence	2			3	2
Reduction degree (%)	<550 °C	550–800 °C	sum	38	106
	55%	35%	90%		

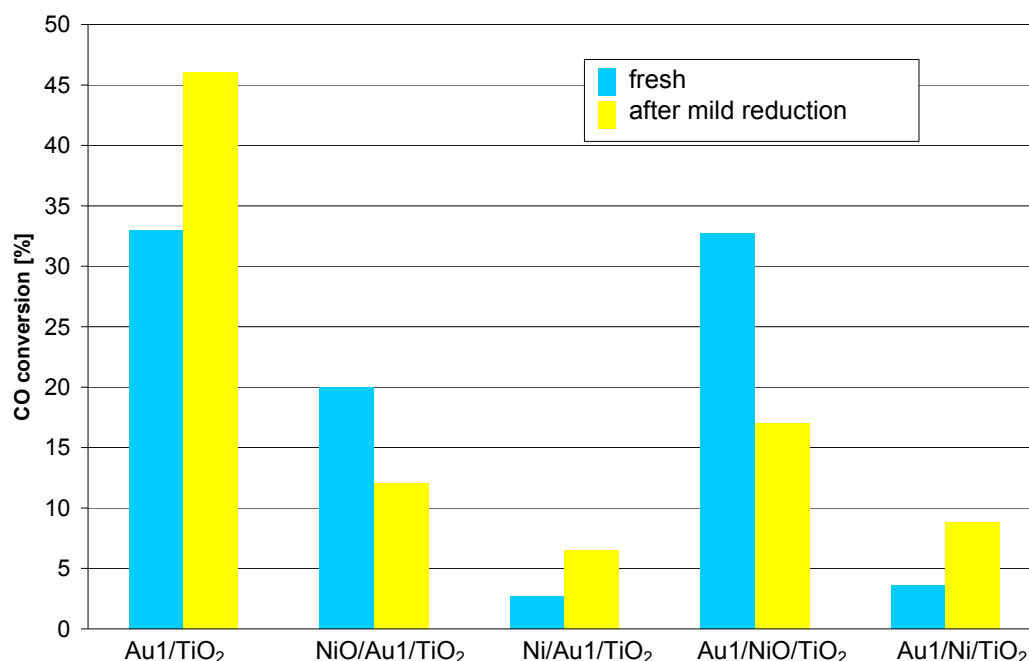
The presented data show that only copper is reduced completely. Iron reduction degree equal to 38% (which is close to 1/3) suggests that the reduction of the Fe³⁺ ion proceeds only up to Fe²⁺. Reduction of pure iron oxides shows that metallic iron is formed at 600 °C at the latest [16]. The reason why iron in the catalyst is not completely reduced may be due to an incorporation of the Fe²⁺ ions in the TiO₂ structure and the creation of a species having much lower reduction equilibrium constant, close to that of ilmenite [17]. It is possible that water vapor generated through the reduction of other species inhibits the reduction of the iron containing species.

The TPR curve of the nickel promoted catalyst and the calculated reduction degree show that below 550 °C half of the nickel is reduced, but above that temperature the reduction intensity is higher than for the reference catalyst. One explanation for that fact could be simply the continuation of the reduction process of nickel oxide. It can be due to an enhanced reduction of titania owing to an increase of the concentration of hydrogen atoms, activated not only on gold nanoparticles but also on the freshly emerged metallic nickel surface.

2.2. Catalytic Results of Catalysts Obtained by Deposition of Reduced or Oxidized Nickel Species on TiO₂ Before and After Gold Nanoparticle Deposition

The catalytic results presented in Figure 2 show the differences between catalysts modified with nickel. The catalysts differ in the order of gold and nickel compound deposition and also in the atmosphere (oxidizing or reducing) the catalysts were heated after nickel compound deposition.

Figure 2. Catalytic activity at 35 °C measured for catalysts differing in the sequence of gold and nickel compound deposition and in the preparation atmosphere (oxidizing or reducing). Reaction conditions: contact time: 0.36 s, feed composition CO:O₂:He ≈ 1:8:24.



The results show that the fresh Au1/NiO/TiO₂ catalyst has a similar activity to the reference catalyst (Au1/TiO₂), but the activity of the fresh NiO/Au1/TiO₂ catalyst is much lower. At the same time the Ni/Au1/TiO₂ catalyst shows a slightly lower activity than the Au1/Ni/TiO₂ catalyst. It appears then that the deposition of gold after nickel compound results in better catalytic activity. On the other hand the catalysts prepared in reducing atmosphere (Au1/Ni/TiO₂, Ni/Au1/TiO₂), exhibit in both cases an activity lower than the reference catalyst. Their activity is also lower than the activity of the respective catalysts prepared in oxidizing atmosphere (Au1/NiO/TiO₂, NiO/Au1/TiO₂). This comparison shows that the preparation in reducing atmosphere at 350 °C generates, irrespective of the Au and Ni deposition sequence, worse catalysts, caused probably by nickel oxide and titania reduction.

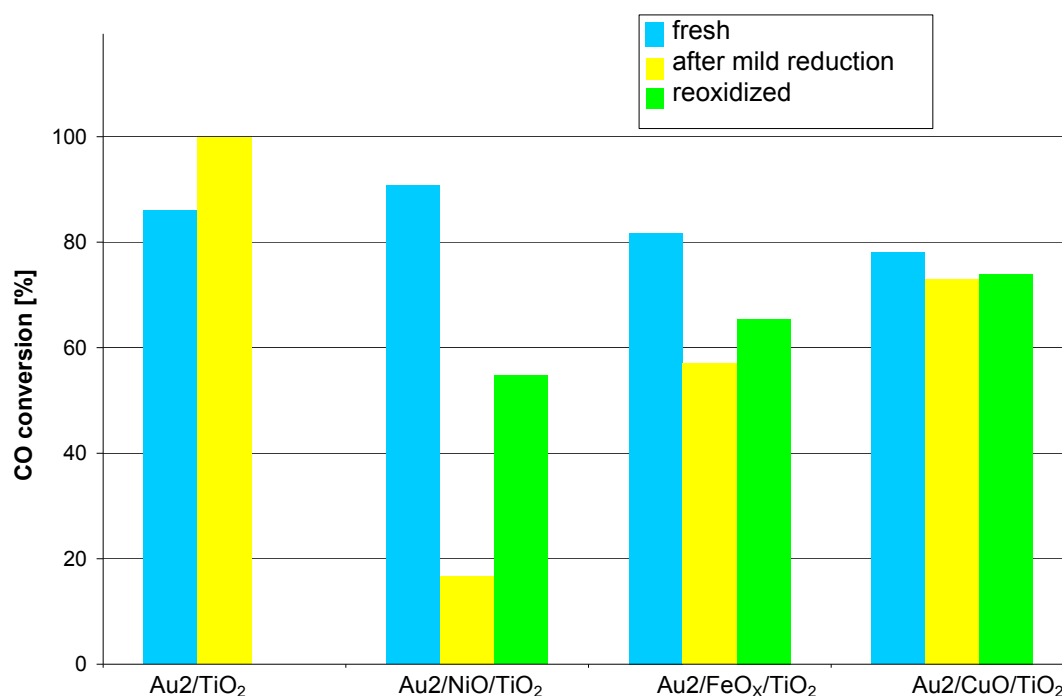
The catalysts react diversely to the mild reduction process (150 °C H₂, 1 h). The activity of the NiO containing catalysts decreases but the Ni containing catalysts become more active. For the Au/TiO₂ reference catalyst, the activity also increases after the mild reduction. As this phenomenon is observed not only for nickel promoted catalysts, this problem will be discussed later.

2.3. Catalytic Results of Catalysts Obtained by Deposition of Base Metal Oxides (Ni, Cu, Fe) on TiO₂ Followed by Gold Nanoparticle Deposition

The bar graph in Figure 3 compares the catalytic activity at 35 °C (conversion at higher temperatures was 100% in all cases) of catalysts promoted with different metals obtained by sequential deposition method. The activity data are given for fresh samples and after mild reduction at 150 °C, followed by reoxidation at 300 °C. As seen, the activity of all the fresh samples was comparable and it can be juxtaposed as follows:



Figure 3. Catalytic activity at 35 °C measured for catalysts obtained by deposition of metal oxides (Ni, Fe, Cu) on TiO₂ before gold nanoparticle deposition. Reaction conditions: contact time: 0.36 s, feed composition: CO:O₂:He ≈ 1:8:24.



There were several articles published in the literature concerning CO oxidation on catalysts obtained by doping of the Au/TiO₂ catalyst with base metals [18–22]. In some cases, the effect is positive, sometimes it is negative or no effect is observed. The results of the group of Sheng Dai [18] show that the doping with NiO improves the catalytic activity. In case of CuO and Fe₂O₃ doped samples, the activity was worse. However it is necessary to take into consideration the content of the dopant metal, which was approximately 10 times higher than in our research. The same content of iron oxide, presented in the paper of Moreau and Bond [19], resulted in the same catalytic activity as the undoped catalyst. A wider spectrum of dopant content is presented in the paper of Parida *et al.* [21], which showed 5% iron content to be the best among 1, 3 and 7%. However, the NaBH₄ preparation method, which resulted in a generally low activity, also makes these results incomparable with ours. Solely the investigations published by Carretin *et al.* [22] presented a catalyst where the surface concentration of iron was close to our catalyst. The synthesized 0.56% Fe-doped Au/TiO₂ catalysts showed several times better activity than the WGC (World Gold Council) reference catalyst (unfortunately the authors did not compare the doped sample with a self-synthesized reference catalyst). The authors ascribed the extraordinary activity to an increase of the number of oxygen defect sites reacting with molecular oxygen to form peroxide and superoxide species. Our TPR experiments suggest that the surface of the iron doped catalyst is more reducible than the surface of the reference catalyst so also in this catalyst more defect sites should be generated. However, the predicted phenomenon was not observed in our research.

The influence of the hydrogen treatment is different: the activity of the reference catalyst (Au₂/TiO₂) increased but that of the promoted catalysts decreased. The strongest effect was observed for the nickel promoted catalyst. In case of the iron promoted one, the impact was moderate and the

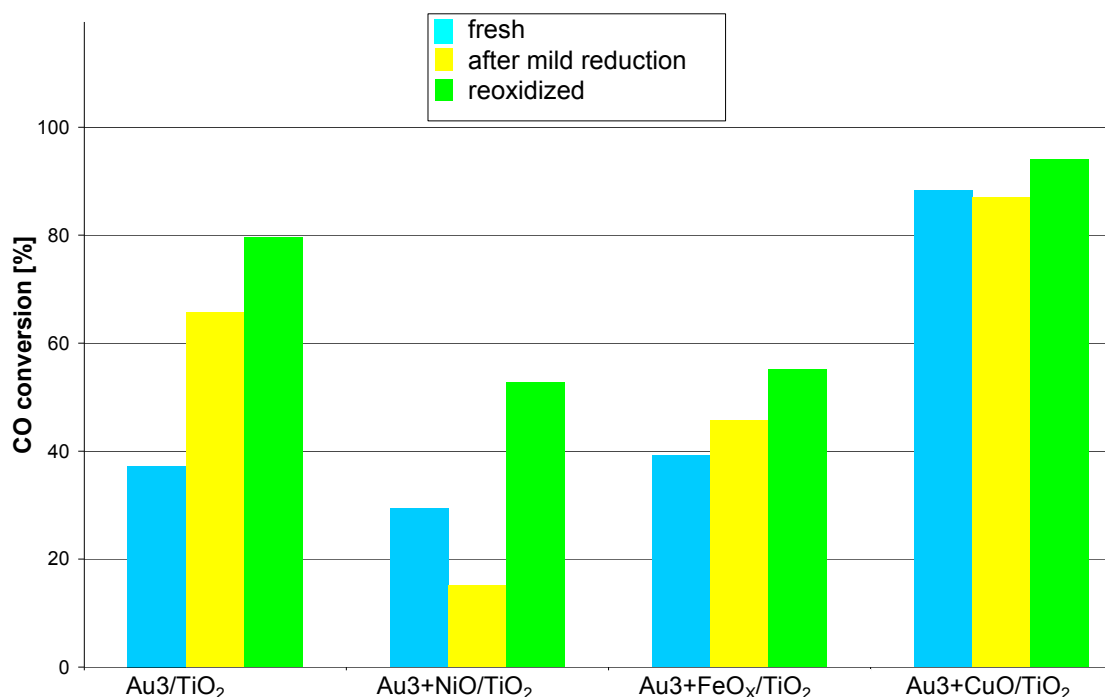
activity of the copper promoted catalyst decreased only slightly. The following reoxidation process improved all promoted catalysts but the initial activity was not restored for any of them.

2.4. Catalytic Results of Catalysts Obtained by Co-deposition of Base Metal Oxides with Oxidized Gold Compounds on TiO_2

The activity of the co-deposited fresh catalysts, measured at 35 °C (Figure 4) is generally much lower than that of the catalysts prepared by sequential deposition. The copper promoted catalyst surpasses the rest of that series, showing a higher conversion of 20%. The conversions measured at higher temperatures kept the same dependencies between the samples as these measured for 35 °C so the data were not plotted.

The mild reduction process (150 °C, H_2/Ar , 1 h) significantly decreased the activity only in the case of $\text{Au}_3 + \text{NiO}/\text{TiO}_2$ while in the case of the copper promoted one ($\text{Au}_3 + \text{CuO}/\text{TiO}_2$) it remained practically stable. In contrast, the activity of the other catalysts clearly increased (Au_3/TiO_2 , $\text{Au}_3 + \text{FeO}_x/\text{TiO}_2$). The reoxidation process increased the activity in all cases especially that of Au_3/TiO_2 , $\text{Au}_3 + \text{NiO}/\text{TiO}_2$, $\text{Au}_3 + \text{FeO}_x/\text{TiO}_2$. The increase after the mild reduction, in the case of copper promoted catalysts, was hardly noticeable. This catalyst series has an exceptional feature *i.e.*, the activity increases after treatments in various conditions. This behavior suggests that the active phase of the catalyst ($\text{Au} + \text{MO}_x$) forms during individual steps of the experiment (*i.e.*, mild reduction, reoxidation).

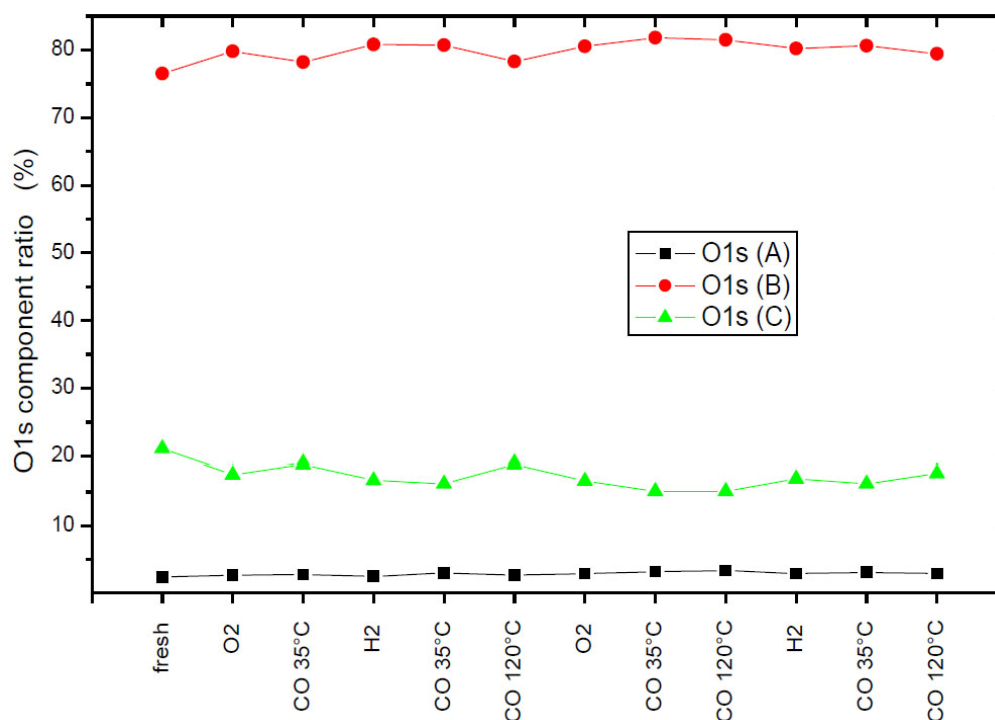
Figure 4. Catalytic activity at 35 °C measured for catalysts obtained by co-deposition of gold and base metal compounds (Ni, Fe, Cu) on TiO_2 . Reaction conditions: contact time: 0.36 s, feed composition: $\text{CO}:\text{O}_2:\text{He} \approx 1:8:24$.



2.5. XPS Measurements Performed in an Ultrahigh Vacuum (UHV) Multichamber System Equipped with a High Pressure Reactor

More information regarding the changes on the Au₂/NiO/TiO₂ catalyst surface were obtained by performing catalytic experiments in the UHV-combined catalytic reactor. The diagram in Figure 5 shows that in the course of the experiment, the concentration of oxygen ascribed to hydroxyl groups does not change significantly and the observed small changes cannot be ascribed to any chemical process.

Figure 5. O 1s component line contents. (A) Oxygen bound to a metal of high electronegativity or in defected structures, BE \approx 528.5; (B) Oxygen bound to metal (bulk oxygen), BE \approx 530.2; (C) Oxygen in OH groups adsorbed on a metal or in CO, or in adsorbed organic compounds, BE \approx 531.5.



Next, the changes of the nickel component lines presented in Figure 6 demonstrate no significant changes in the nickel oxidation state from stage to stage of the experiment. The concentration of Ni³⁺ ions (Figure 6a) increases slowly in the course of the process and also—as in the case of oxygen—the changes cannot be ascribed to any specific reaction of the catalyst's surface with the applied gas phase. The gold component lines presented in Figure 7 demonstrate more variable behaviour. During the first six steps, only the BE of the cationic gold is changed, while the other binding energies remain stable. After the reoxidation process the BE values of the B and C curves change. The observed changes suggest a polarization of the surface due to CO adsorption and desorption rather than changes in the state of gold. This experiment clearly shows that the particular steps of the process do not generate distinct changes in the state of nickel or gold themselves, but it can be rather expected that the interactions between these elements could change due to reduction of titania. The TPR experiment confirms the fact that no changes in nickel oxidation state are observed up to 150 °C.

Figure 6. Ni 2p component line behaviour. A: Ni²⁺ (NiO), B: Ni³⁺, C: Ni²⁺ in salts or the Ni^{x+}-TiO₂ interface (a) Binding energy changes; (b) Contents of various Ni species.

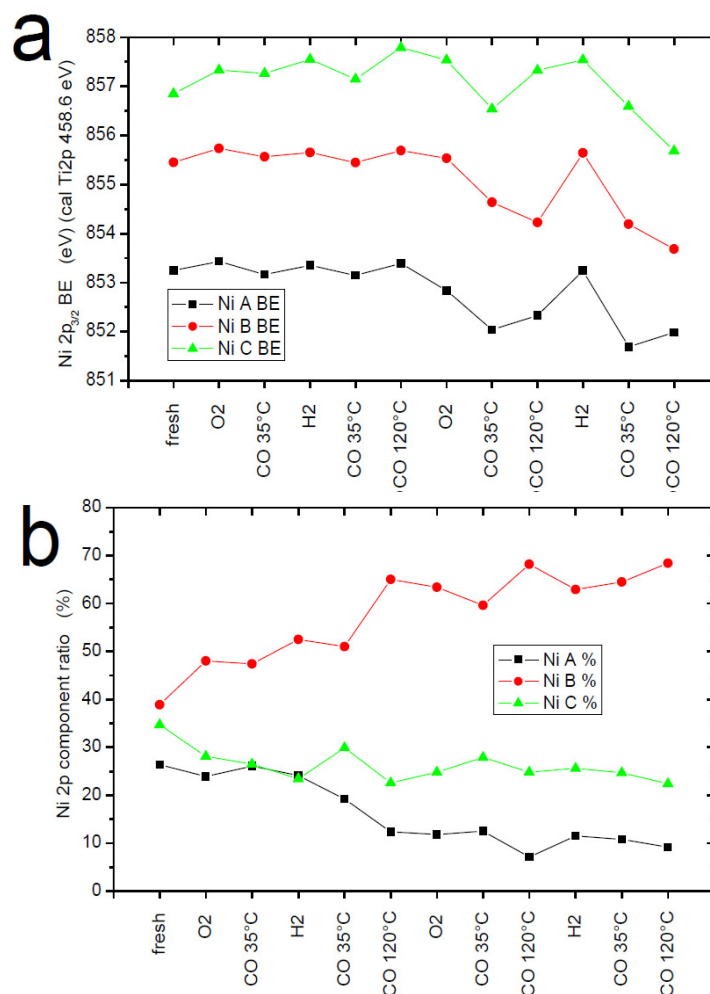


Figure 7. Au 4f component line behaviour. A: anionic gold (Au^{-δ}), B: metallic gold (Au⁰), C: cationic gold (Au^{+δ}) (a) Binding energy changes; (b) Contents of various Au species.

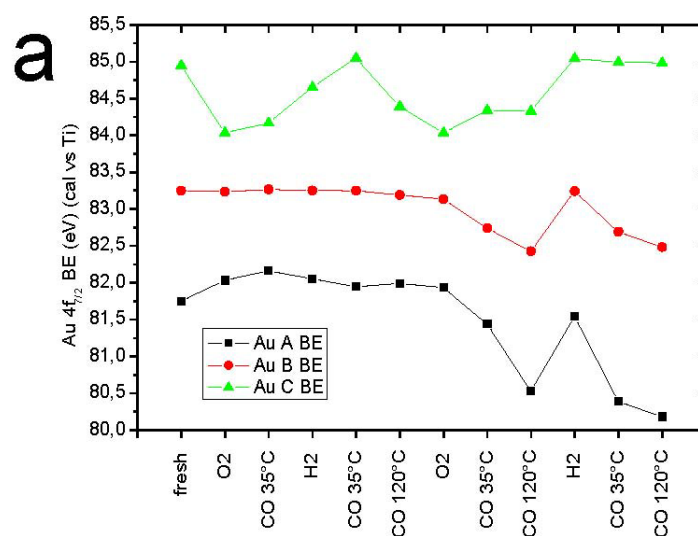
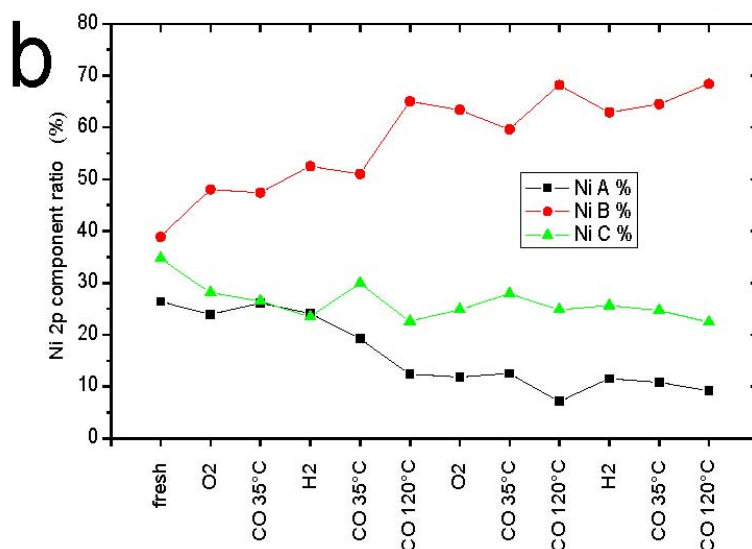


Figure 7. Cont.



2.6. The Influence of the Mild Reduction Process (150 °C, H₂/Ar, 1 h)

It has been shown in many articles that treatments in oxidizing or reducing atmospheres had a remarkable impact on gold catalysts. Some of these papers claim a positive effect of the hydrogen treatment; others report an activity decrease after this treatment [23–25].

The presented catalytic results show that the mild reduction process has also a marked influence on all catalysts' activities. Promoted catalysts, obtained by sequential deposition method and prepared in oxidizing atmosphere, lost their activities while the catalysts prepared in reducing atmosphere improved after this process (Figures 2 and 3). However, the unpromoted catalysts of each series (Au1, Au2, Au3) were enhanced.

The co-deposited catalysts reacted more intricately to the mild reduction process: it was observed that it decreased significantly the activity only in the case of Au₃ + NiO/TiO₂, for the iron promoted catalyst (Au₃ + FeO_x/TiO₂) the activity increased, while in the case of the copper promoted one (Au₃ + CuO/TiO₂), it remained practically stable. It was stated in Section 2.4 that the active phase of the co-deposited catalysts (Au + MO_x) develops along individual steps of the experiment (*i.e.*, mild reduction, reoxidation). From this it follows that the performed hydrogen treatment changes the catalyst surface (as is observed for the sequentially deposited catalysts) as well as generating the aforementioned active phase development. Hence, due to the active phase development, this catalyst series does not provide reliable data about the changes on the catalyst surface so the behavior of the co-deposited catalysts will not be further taken into consideration.

The first thing that needs to be dealt with is the different influence of hydrogen on the unpromoted catalysts and the promoted ones prepared in oxidizing atmosphere. A possible explanation of this difference is the formation of surface titanate phases [26] in the promoted catalysts, and these titanate phases are less reducible than anatase, so the formation of oxygen vacancies is more difficult. Since the mild reduction has the strongest influence on the nickel promoted catalyst, weaker on iron and the weakest on the copper promoted one, it can be concluded that these metals are incorporated into the TiO₂ to a different extent. The higher the activity decrease, the more the dopant metal incorporated

into the TiO₂ structure. It is also possible that the activity decrease is not a question of higher or lower incorporation, but rather a feature of the particular titanate phases and their reducibility.

Additional questions provide the catalytic results of catalysts obtained by the preparation in reducing atmosphere. As shown in Figure 2, the influence of the mild reduction process is positive, which makes these catalysts similar to the unpromoted one.

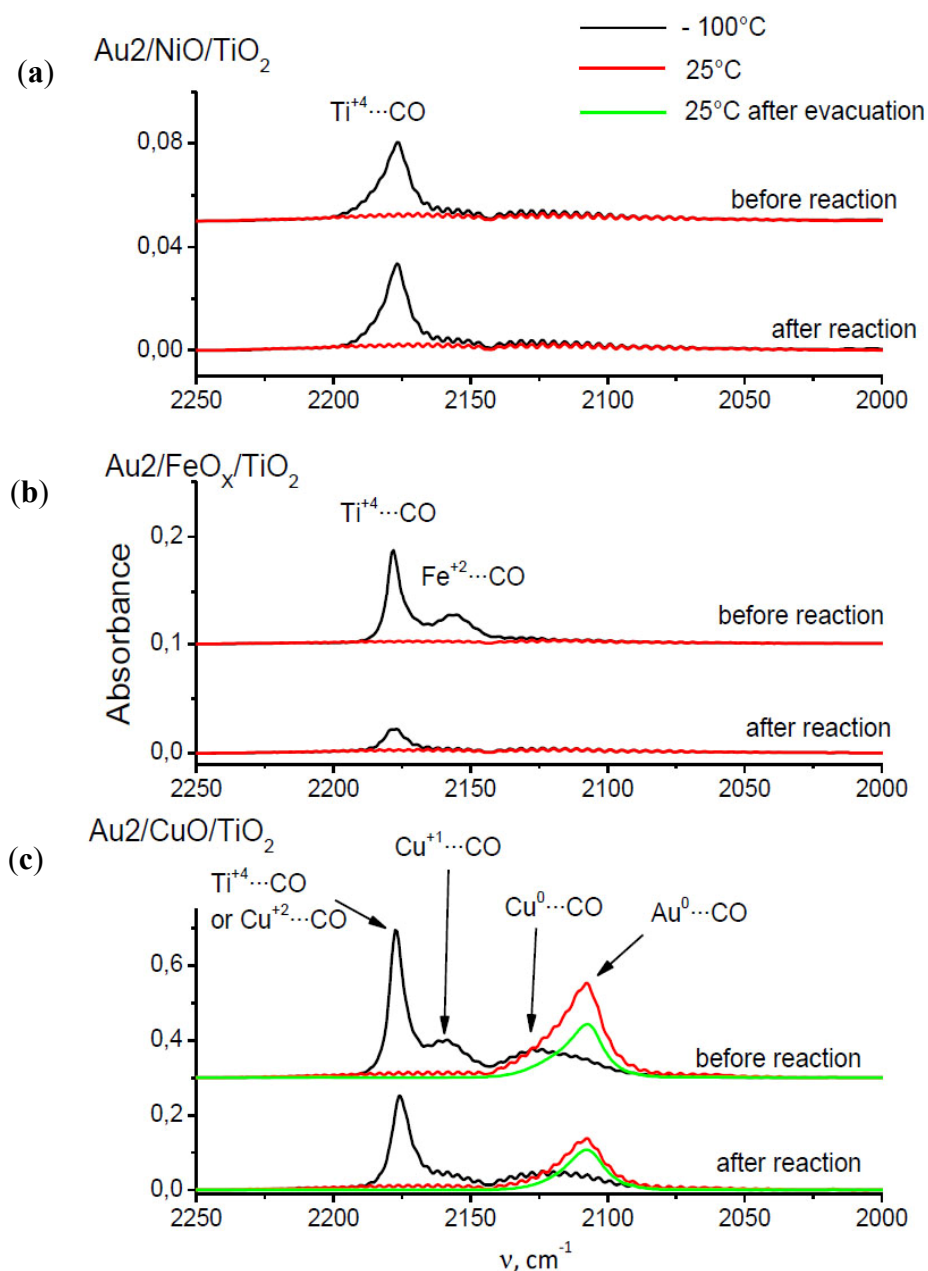
A possible explanation for the diverse behaviors of all the investigated samples could be the twofold influence of the mild reduction on the catalytic system. Firstly, hydrogen reduces Au cations creating a more active species [27,28] or generates hydroxyl groups on the gold nanoparticle perimeter [29,30], resulting in an activity increase. Secondly, hydrogen reduces surface oxygen species making the support unable to donate oxygen species [31–33], which results in an activity decrease. Based on these two assumptions, it can be suggested that, in the case of the promoted catalysts prepared in oxidizing atmosphere, both phenomena occur. In each case hydrogen generates a positive effect according to the first assumption. However depending on the aforementioned titanates formation and their different content or reducibility, hydrogen decreases the catalytic activity. In these catalysts containing the dopant metal in oxidized form, both phenomena compete, so the resultant activity depends on the extent of these two particular phenomena.

The unpromoted reference catalyst which does not contain any titanate phases is not negatively influenced due to the support reduction so the only effect which is observed is the positive effect. On the other hand, in the case of catalysts prepared in reducing atmosphere (350 °C), the support underwent a deep reduction generating a surface structure which is less abundant in free oxygen species. Then, during the mild reduction process (150 °C), the support cannot be reduced anymore, so the hydrogen treatment can only influence gold nanoparticles or generate hydroxyl groups (according to the first assumption).

2.7. Catalysts Surface Changes Observed with FTIR

Further data indicating the changes inside the support were obtained by FTIR. The spectra collected for Au₂/NiO/TiO₂, Au₂/FeO/TiO₂, Au₂/CuO/TiO₂ samples are plotted in Figure 8. Each diagram consists of two sets of spectra where the upper one refers to the sample before catalytic reaction (heating at 120 °C in a CO–O₂–He mixture) and the lower one, after it. According to the literature [34,35], the observed frequencies were attributed to CO adsorption on the following centers: 2175 cm⁻¹—weak Lewis centers on Ti⁺⁴ (β-center) [35] and/or Cu⁺², 2158 cm⁻¹—Cu⁺¹, 2156 cm⁻¹—Fe⁺², 2127 cm⁻¹—Cu⁰, 2108 cm⁻¹—Au⁰.

Figure 8. Comparison of CO adsorption FTIR spectra of Au/TiO₂ catalysts promoted by (a) Ni; (b) Fe; (c) Cu.



The presented spectra show that CO adsorbs on the Ti⁴⁺ β -centers (2175 cm⁻¹) at -100 °C in the case of each catalyst, but the peak intensity is different for each catalyst and also depends on whether CO was adsorbed on the catalyst before or after reaction. For the Au₂/NiO/TiO₂ catalyst, the peak intensity before and after the catalytic reaction, is comparable and amounts to about 0.036 a.u. The height of this peak in the case of the Au₂/FeO/TiO₂ catalyst before the reaction is about three times higher than for Au₂/NiO/TiO₂, but after the reaction it is comparable to the peak height of Au₂/NiO/TiO₂. For the Au₂/CuO/TiO₂ catalyst, the intensity of this peak cannot clearly be determined due to the fact that the vibration of CO adsorbed on Cu²⁺ has a similar frequency. However, it can be concluded that the intensity of the band before the reaction is nearly 1.6 times higher than after the reaction.

The spectra of CO adsorption on the catalyst Au₂/NiO/TiO₂ do not show any characteristic vibrations, with the exception of the aforementioned CO-β (Ti⁺⁴) vibration centers. The adsorption of CO on Au₂/FeO/TiO₂ leads to the appearance of the 2162 cm⁻¹ band which can be attributed to the interaction of CO with Fe⁺². In the Au₂/CuO/TiO₂ spectra, besides the CO-β-centers vibration, two additional bands 2168 cm⁻¹ and 2127 cm⁻¹ were recorded at -100 °C, which correspond to the CO-Cu⁺¹ and CO-Cu⁰ vibrations respectively. At room temperature a broadened peak appears, consisting probably of two vibrations 2127 cm⁻¹-Cu⁰ and 2108 cm⁻¹, attributed to CO-Au⁰ vibration [35]. For this catalyst, such dependencies can be stated:

(a) CO-Cu⁰ vibration is observed at both temperatures (-100 °C and room temperature).

(b) the assignment of 2108 cm⁻¹ frequency to CO-Au⁰ vibration, although it has its justification in the literature, seems to be questionable because at the same time it should be observed for other catalysts.

(c) the ratio of peaks at 2175 cm⁻¹ recorded in the spectra before and after the reaction is approximately equal to the ratio of peaks at 2108 cm⁻¹ in the spectra collected before and after the reaction, which may indicate that the catalytic reaction leads to a decrease of the amount of both adsorption centers in a uniform extent.

A general feature, which is common for the iron and the copper promoted catalyst, is the lower absorbance before reaction for all frequencies. The nickel promoted catalyst exhibits low peaks before and after reaction.

2.8. Comparison of Preparation Methods

Comparison of the preparation methods showed that the gold after metal sequential deposition method is better than the metal after gold sequential deposition method and, in most cases, is also better than the co-deposition method. However the co-deposited copper promoted catalyst exhibited the highest activity of all the prepared samples.

3. Experimental Section

Titanium dioxide (100% anatase [36]) from TIOXIDE with specific surface area of 32 m²g⁻¹ or 22.4 m²g⁻¹ was used as support. Au/MO_x/TiO₂ and MO_x/Au/TiO₂ systems were synthesized by sequential deposition of each component but in different order. Gold nanoparticles were deposited through deposition-precipitation method (DP), using ammonium hydroxide at pH = 9.0 as precipitating agent and chloroauric acid as Au source. Metal oxides were deposited by impregnation of the support with nitrates (Cu, Fe) or ammonates (Ni) followed by heating at 350 °C in oxidizing or reducing atmosphere. The nominal concentration of gold is 1 wt% and the amount of the additive metal is equimolar.

Au-MO_x/TiO₂ systems were obtained by co-deposition of gold and base metal compounds on the support. The applied method was similar to the DP method, but a mixture of chloroauric acid and a base metal chloride was used instead of chloroauric acid only.

The specific surface areas of the samples were determined with the use of Quantachrome–Autosorb-1 instrument. Samples were degassed at 150 °C under vacuum (10^{-6} mmHg). N₂ was used as adsorbate at 77.4 K. BET isotherm was used to determine the specific surface area.

The surface composition and texture study was performed using a high resolution scanning electron microscope JEOL JSM-7500F with extra-INCA EDS PentaFETx3. Secondary electron imaging detector-SEI was used to determine the catalyst morphology, for gold particles imaging on the catalyst surface Back-Scattered Electron detector-BSE was used.

Catalyst reducibility measurements were carried out with the use of Quantachrome Chembet-3000 apparatus, in a flow of 30 mL/min of 5% H₂/Ar mixture. The amount of the sample (0.68 g) was selected in such a way that limitations by heat and mass transfer were avoided and good resolution was obtained. The heating rate was 10 °C/min. Water vapor was removed by freezing. Reduction peak maximum T_{max} was the reducibility describing factor.

FT-IR spectra were recorded in absorption mode on a Bruker Tensor 27 spectrometer equipped with a MCT detector, with a spectral resolution of 2 cm⁻¹. The cuvette was connected online to a gas feed system and equipped with a temperature control system to perform measurements from –100 to 150 °C in controlled atmosphere at pressures of 10⁻⁴ to 1 bar. The measurement was carried out according to the following procedure:

1. Degassing under vacuum at 150 °C;
2. CO adsorption at –100 °C and collecting FTIR spectra;
3. Warming up up to room temperature and collecting FTIR spectra;
4. Degassing and collecting FTIR spectra;
5. Catalytic reaction in 2% CO, 2% O₂/He atmosphere at 100 °C for 4 h;
6. Collecting FTIR spectra like in points 2–4.

The catalytic experiments were performed in a stainless steel reactor (i.d. = 8 mm, h = 19 mm) connected online with an SRI 8610C Gas Chromatograph equipped with two columns for reactant analysis. Helium Ionization Detector (HID) was used for CO and O₂ analysis. The elution of them was performed on a packed column with 13X molecular sieves. CO₂ analysis was performed on a Porapak Q column connected to a TCD detector. The gas feed was controlled by β-ERG Mass Flow Controllers. The feed gas mixture total flow was 58 mL/min and its composition was CO—3%, O₂—24%, He—73%. The amount of the catalyst was approximately 0.33 g. The catalytic experiments were performed according to the following steps:

1. Standardizing (oxidation at 150 °C in O₂/He for 1 h);
2. Catalytic CO oxidation at 35, 50 and 60 °C;
3. Mild reduction at 150 °C in H₂/He for 1 h;
4. Catalytic CO oxidation at 35, 50 and 60 °C;
5. Reoxidation at 300 °C in O₂/He for 1 h;
6. Catalytic CO oxidation at 35, 50 and 60 °C.

In case of Au₁/TiO₂ catalyst and its modification (Figure 2), the steps 1–4 were only performed and the catalytic activity was measured only at 35 °C. All of the catalyst prepared by gold after metal

sequential deposition method (Figure 3) exhibited 100% conversion at temperatures 50 and 60 °C so the diagram shows only the results obtained at 35 °C.

XPS studies were carried out in an ultrahigh vacuum (UHV) multichamber system equipped with a high-pressure reactor (Prevac). A pellet of powdered sample was placed on a holder containing resistive heater covered with ceramic coating. The experiments were carried out according to the following procedure:

1. Standardizing (oxidation at 150 °C in O₂/He for 1 h);
2. Catalytic CO oxidation at 35 °C;
3. Mild reduction at 150 °C in H₂/He for 1 h;
4. Catalytic CO oxidation at (a) 35 °C (b) 120 °C;
5. Reoxidation at 300 °C in O₂/He for 1 h;
6. Catalytic CO oxidation at (a) 35 °C (b) 120 °C;
7. Mild reduction at 150 °C in H₂/He for 1 h;
8. Catalytic CO oxidation at (a) 35 °C (b) 120 °C.

The sample was not active until the catalytic reaction at 120 °C was performed, so the steps 7 and 8 were carried out as a repetition. For the standardizing and reoxidation processes a mixture of 5% O₂/He 30 mL/min was used. The mild reduction process was carried out with 33% H₂/He. The feed mixture used in the CO oxidation process contained 2% CO, 2% O₂ in He. At every step the gas flow was 30 mL/min and the reaction temperature was monitored by a thermocouple attached to the sample. The reaction progress was followed qualitatively by mass spectrometer (SRS 200), linked to the reactor by registering masses 2, 12, 16, 18, 32, 40, 44 and 48. After each treatment, the sample was cooled down, the reactor was evacuated to 2×10^{-7} mbar and then the sample was transferred to the XPS spectrometer chamber (5×10^{-10} mbar). The XPS measurements were performed with Al K α (1486.6 eV) X-ray source and hemispherical analyzer R4000 (Gammadata Scienta). The spectrometer was calibrated according to ISO 15472:2001. The energy resolution of the system, measured as a full width at half maximum (FWHM) for Ag 3d_{5/2} excitation line, was 0.9 eV. Titanium 2p_{3/2} core excitation at binding energy of 458.6 eV, was taken as an internal standard. The assignment of the obtained BE values was done basing on references [37–39].

The spectra were processed in CasaXPS 2.3.12 program. In the spectra, the background was approximated by a Shirley profile. The spectra deconvolution into a minimum number of the components was done by application of the Voigt-type line shapes (70:30 Gaussian/Lorentzian product).

4. Conclusions

The presented results show that doping of the gold/titania catalyst with copper, iron and nickel results in obtaining samples with quite diverse properties. Firstly, they reveal different redox properties. The reducibility of the copper promoted gold catalyst is the highest, the iron promoted one has a slightly lower reducibility and that of the nickel promoted catalyst is the lowest. The redox behavior was attributed to the extent of incorporation of the dopant metals into the titania structure.

The activity of the fresh catalysts was comparable (with the exception of the catalysts prepared by Metal after Gold Sequential Deposition) but the mild reduction process demonstrated distinct

differences: nickel promoted catalysts lost their activities significantly, while the iron promoted ones lost only slightly; and the influence on the copper promoted one is hardly noticeable. It was concluded that catalytic activity depends considerably on the reducibility of the supports. The formation of surface titanates decreases the amount of free oxygen species.

The FTIR investigation showed a higher concentration of active sites adsorbing CO on iron and copper promoted catalysts. However, the catalytic reaction reduces the amount of these sites.

From the three presented preparation methods, the gold after metal sequential deposition method seems to be the most effective.

Acknowledgments

This work was supported in part by the Polish Ministry of Science and Higher Education and by the Team Program of the Foundation for Polish Science co-financed by the EU European Regional Development Fund.

The authors wish to acknowledge fruitful discussions with Barbara Grzybowska-Świerkosz.

References

1. Bone, W.A.; Wheeler, R.V. The combination of hydrogen and oxygen in contact with hot surfaces. *Philos. Trans. R. Soc. London Ser. A* **1906**, *206*, 1–67.
2. Benton, A.F.; Elgin, J.C. The catalytic synthesis of water vapor in contact with metallic gold. *J. Am. Chem. Soc.* **1927**, *49*, 2426–2438.
3. Yates, D.J.C. Spectroscopic investigations of gold surfaces. *J. Colloid Interface Sci.* **1969**, *29*, 194–204.
4. Bond, G.; Sermon, P. Gold catalysts for olefin hydrogenation. *Gold Bull.* **1973**, *6*, 102–105.
5. Schwank, J. Gold in bimetallic catalysts. *Gold Bull.* **1985**, *18*, 2–10.
6. Haruta, M.; Kobayashi, T.; Sano, H.; Yamada, N. Novel gold catalysts for the oxidation of carbon-monoxide at a temperature far below 0-degrees-C. *Chem. Lett.* **1987**, *16*, 405–408.
7. Tokumitsu, S.; Nakano, K.; Naruo, N. Removal of malodor. *Japanese Patent JP 05115748*, 14 May 1993.
8. Haruta, M. When gold is not noble: Catalysis by nanoparticles. *Chem. Rec.* **2003**, *3*, 75–87.
9. Ondrey, G. Gold catalyzes a one-step synthesis of methyl glycolate. *Chem. Eng.* **2004**, *20*, 111–173.
10. Knell, A.; Barnickel, P.; Baiker, A.; Wokaun, A. CO oxidation over Au/ZrO₂ catalysts—Activity, deactivation behavior, and reaction-mechanism. *J. Catal.* **1992**, *137*, 306–321.
11. Dobrosz-Gomez, I.; Gomez-Garcia, M.A.; Rynkowski, J.M. CO oxidation over Au/CeO₂-ZrO₂ catalysts: The effect of the support composition of the Au-support interaction. *Kinet. Catal.* **2010**, *51*, 823–827.
12. Lopez, N.; Janssens, T.V.W.; Clausen, B.S.; Xu, Y.; Mavrikakis, M.; Bligaard, T.; Nørskov, J.K. On the origin of the catalytic activity of gold nanoparticles for low-temperature CO oxidation. *J. Catal.* **2004**, *223*, 232–235.
13. Bond, G.; Thompson, D. Gold-catalysed oxidation of carbon monoxide. *Gold Bull.* **2000**, *33*, 41–50.
14. Wang, J.; Hammer, B. Oxidation state of oxide supported nanometric gold. *Top. Catal.* **2007**, *44*, 49–56.

15. Haruta, M. Gold as a novel catalyst in the 21st century: Preparation, working mechanism and applications. *Gold Bull.* **2004**, *37*, 27–36.
16. Zielinski, J.; Zglinicka, I.; Znak, L.; Kaszkur, Z. Reduction of Fe₂O₃ with hydrogen. *Appl. Catal. A* **2010**, *381*, 191–196.
17. Jaime-Albalat, A. Assessment of oxygen production on the moon through reduction of ilmenite. Master Thesis, Technical University of Catalonia, Barcelona, Spain, 2010.
18. Ma, Z.; Overbury, S.H.; Dai, S. Au/MxOy/TiO₂ catalysts for CO oxidation: Promotional effect of main-group, transition, and rare-earth metal oxide additives. *J. Mol. Catal. A Chem.* **2007**, *273*, 186–197.
19. Moreau, F.; Bond, G.C. CO oxidation activity of gold catalysts supported on various oxides and their improvement by inclusion of an iron component. *Catal. Today* **2006**, *114*, 362–368.
20. Shou, M.; Takekawa, H.; Ju, D.-Y.; Hagiwara, T.; Lu, D.-L.; Tanaka, K.-I. Activation of a Au/TiO₂ catalyst by loading a large amount of Fe-Oxide: Oxidation of CO enhanced by H₂ and H₂O. *Catal. Lett.* **2006**, *108*, 119–124.
21. Parida, K.M.; Sahu, N.; Mohapatra, P.; Scurrrell, M.S. Low temperature CO oxidation over gold supported mesoporous Fe-TiO₂. *J. Mol. Catal. A Chem.* **2009**, *319*, 92–97.
22. Carrettin, S.; Hao, Y.; Aguilar-Guerrero, V.; Gates, B.C.; Trasobares, S.; Calvino, J.J.; Corma, A. Increasing the number of oxygen vacancies on TiO₂ by doping with iron increases the activity of supported gold for CO oxidation. *Chem. Eur. J.* **2007**, *13*, 7771–7779.
23. Gupta, N.M.; Tripathi, A.K. Microcalorimetry, adsorption, and reaction studies of CO, O₂, and CO + O₂ over Fe₂O₃, Au/Fe₂O₃, and polycrystalline gold catalysts as a function of reduction treatment. *J. Catal.* **1999**, *187*, 343–347.
24. Guzzi, L.; Horváth, D.; Pászti, Z.; Pető, G. Effect of treatments on gold nanoparticles: Relation between morphology, electron structure and catalytic activity in CO oxidation. *Catal. Today* **2002**, *72*, 101–105.
25. Su, Y.-S.; Lee, M.-Y.; Lin, S. XPS and DRS of Au/TiO₂ catalysts: Effect of pretreatment. *Catal. Lett.* **1999**, *57*, 49–53.
26. De Bokx, P.K.; Bonne, R.L.C.; Geus, J.W. Strong metal-support interaction in Ni/TiO₂ catalysts: The origin of TiOx moieties on the surface of nickel particles. *Appl. Catal.* **1987**, *30*, 33–46.
27. Henao, J.D.; Caputo, T.; Yang, J.H.; Kung, M.C.; Kung, H.H. *In situ* transient FTIR and XANES studies of the evolution of surface species in CO oxidation on Au/TiO₂. *J. Phys. Chem. B* **2006**, *110*, 8689–8700.
28. Costello, C.K.; Kung, M.C.; Oh, H.S.; Wang, Y.; Kung, H.H. Nature of the active site for CO oxidation on highly active Au/Al₂O₃. *Appl. Catal. A* **2002**, *232*, 159–168.
29. Costello, C.K.; Yang, J.H.; Law, H.Y.; Wang, Y.; Lin, J.N.; Marks, L.D.; Kung, M.C.; Kung, H.H. On the potential role of hydroxyl groups in CO oxidation over Au/Al₂O₃. *Appl. Catal. A* **2003**, *243*, 15–24.
30. Molina, L.M.; Hammer, B. Some recent theoretical advances in the understanding of the catalytic activity of Au. *Appl. Catal. A* **2005**, *291*, 21–31.
31. Schubert, M.M.; Hackenberg, S.; van Veen, A.C.; Muhler, M.; Plzak, V.; Behm, R.J. CO oxidation over supported gold catalysts—“Inert” and “Active” support materials and their role for the oxygen supply during reaction. *J. Catal.* **2001**, *197*, 113–122.

32. Liu, H.; Kozlov, A.I.; Kozlova, A.P.; Shido, T.; Asakura, K.; Iwasawa, Y. Active oxygen species and mechanism for low-temperature CO oxidation reaction on a TiO₂-supported Au catalyst prepared from Au(PPh₃)(NO₃) and As-precipitated titanium hydroxide. *J. Catal.* **1999**, *185*, 252–264.
33. Grzybowska-Świerkosz, B. Nano-Au/oxide support catalysts in oxidation reactions: Provenance of active oxygen species. *Catal. Today* **2006**, *112*, 3–7.
34. Zhang, T.; Liu, X.Y.; Wang, A.Q.; Li, L.; Mou, C.Y.; Lee, J.F. Structural changes of Au-Cu bimetallic catalysts in CO oxidation: *In situ* XRD, EPR, XANES, and FT-IR characterizations. *J. Catal.* **2011**, *278*, 288–296.
35. Kondarides, D.I.; Panagiotopoulou, P.; Verykios, X.E. Mechanistic study of the selective methanation of CO over Ru/TiO₂ catalyst: Identification of active surface species and reaction pathways. *J. Phys. Chem. C* **2011**, *115*, 1220–1230.
36. Grzybowska, B.; Słoczyński, J.; Grabowski, R.; Samson, K.; Gressel, I.; Weisło, K.; Gengembre, L.; Barboux, Y. Effect of doping of TiO₂ support with altermultivalent ions on physicochemical and catalytic properties in oxidative dehydrogenation of propane of vanadia—Titania catalysts. *Appl. Catal. A* **2002**, *230*, 1–10.
37. Wanger, C.D.; Riggs, W.M.; Davis, L.E.; Moulder, J.F.; Muilenberg, G.E. *Handbook of X-ray Photoelectron Spectroscopy*; Perkin-Elmer Corporation: Eden Prairie, MN, USA, 1992; p. 190.
38. Wagner, C.D.; Naumkin, A.V.; Kraut-Vass, A.; Allison, J.W.; Powell, C.J.; Rumble, J.R., Jr. *X-Ray Photoelectron Spectroscopy Database*; NIST Standard Reference Database 20, Version 3.5, 6 June 2000. Available online: <http://srdata.nist.gov/xps> (accessed on 11 May 2011).
39. *Electron Spectroscopy Database*; Thermo Fisher Scientific: Courtaboeuf Cedex, France. Available online: <http://www.lasurface.com> (accessed on 11 May 2011).

© 2012 by the authors; licensee MDPI, Basel, Switzerland. This article is an open access article distributed under the terms and conditions of the Creative Commons Attribution license (<http://creativecommons.org/licenses/by/3.0/>).